

***In situ* Synthesis of CuS Nanoparticle Doped Poly(N-isopropylacrylamide)-Based Microgels for Near Infrared Triggered Photothermal Therapy**

Tong Shu,^{a,b} Qiming Shen,^b Lei Su^a, Xueji Zhang^a and Michael J. Serpe*^b

^a Beijing Advanced Innovation Center of Materials Genome Engineering, Beijing Key Laboratory for Bioengineering and Sensing Technology, Research Center for Bioengineering and Sensing Technology, University of Science and Technology Beijing, Beijing 100083, P. R. China;

^bDepartment of Chemistry, University of Alberta, Edmonton, Alberta, T6G 2G2, Canada.

Department of Chemistry, University of Alberta, Edmonton, Alberta, Canada T6G

2G2. E-mail: michael.serpe@ualberta.ca;

Fax: +1 780 492 8231; Tel: +1 780 492 5778

Abstract

Poly (N-isopropylacrylamide)-co-(acrylic acid) (pNIPAm-co-AAc) microgels incorporated with CuS nanoparticles (CuSNPs) were synthesized and employed for near infrared (NIR) triggered photothermal killing of cancer cells. Cu^{2+} was enriched in the microgels through deprotonation of the pNIPAm-co-AAc microgels at high solution pH. CuSNPs were subsequently generated within the pNIPAm-co-AAc microgels upon exposure to heat and S^{2-} . The solution of hybrid microgels showed an absorption peak in the NIR region (~ 1000 nm). After demonstrating that the hybrid microgels were not cytotoxic, we showed that NIR excitation of the hybrid microgels could be used to kill HeLa cells. Almost 90% HeLa cells were killed when incubated with 400 $\mu\text{g/mL}$ of the hybrid microgels and exposed to 808 nm laser light with a power density of 2 W/cm^2 for 10 min. While these materials show promise for photothermal therapy, they can also be incorporated into a hydrogel matrix that can be triggered to release small molecule drugs upon exposure to NIR wavelengths.

Keywords: Photothermal therapy; Poly(N-isopropylacrylamide)-co-(acrylic acid) microgels; CuS nanoparticles; Near infrared excitation

Introduction

Electromagnetic stimulation of processes using near infrared (NIR) radiation in the wavelength range of 700-1100 nm has become extremely important for photothermal therapy due to the ability of these wavelengths to penetrate skin.¹ Furthermore, NIR wavelengths can selectively stimulate these processes without the side effects of some other wavelengths of electromagnetic radiation, and are minimally invasive.²⁻³ As such, NIR-enabled therapies have been used as novel alternatives for carcinoma treatment.⁴⁻⁶ Recently, many investigations have focused on new therapeutic methods that utilize novel photothermal materials/agents. Relatedly, a variety of materials/agents capable of NIR-triggered heating have been identified, such as organic dyes,⁷ gold nanostructures,⁸ carbon composites,⁹ and palladium nanosheets.¹⁰ Of interest to the study here are CuS nanomaterials that are known for their localized surface plasmon resonances at NIR wavelengths,¹¹ low cytotoxicity, environmentally friendly synthesis, and low cost.¹² Among the family of CuS nanomaterials, spherical CuS nanoparticles are the most commonly used due to their facile synthesis and relatively high NIR-heat conversion efficiency.¹³ However, due to their high specific surface area, CuS nanoparticles (CuSNPs) are not colloidally stable, and readily aggregate and precipitate in solution. Thus, surface modification of CuSNPs has been used to stabilize the particles and prevent their aggregation. CuSNPs surface modification can also yield many new properties, e.g., the ability to specifically bind to cancer cells by modification with folic acid.¹⁴

Since their discovery, stimuli-responsive polymers have been used for a variety of applications mainly due to their ability to "sense" their environment and "react" to it chemically and/or physically.¹⁵⁻¹⁶ Of the various stimuli responsive polymers, poly(N-isopropylacrylamide) (pNIPAm) has received the most attention, and has also been used to stabilize nanoparticles.¹⁷⁻¹⁸ pNIPAm is well known to exhibit thermoresponsivity, exhibiting a lower critical solution temperature (LCST) and collapsing/deswelling above 32 °C in water. The deswelling/reswelling process is fully reversible over many cycles. PNIPAm-based networks can also be generated via

polymerization in the presence of a crosslinker. Furthermore, colloiddally stable pNIPAm-based nano and micro particles (nanogels/microgels, respectively) can also be generated,¹⁹ and multiple responsivities can be introduced into the microgels via copolymerization with functional monomers.²⁰⁻²¹ While these additional functional monomers have been used to render pNIPAm-based materials responsive to multiple stimuli, they have also been used to introduce nanomaterials into their network structure.²² For instance, pNIPAm microgels have been loaded with photothermal nanomaterials, i.e., reduced graphene oxide nanoparticles¹⁸ and gold nanorods,²³ via simple mixing. The hybrids thus display light responsivity by changing their solvation state, which can be exploited for drug delivery in biological systems.²⁴ Functionalized pNIPAm-based microgels can also see as microreactors for the synthesis of nanoparticles. Specifically, in a previous study, we showed that pNIPAm-co-acrylic acid (pNIPAm-co-AAc) microgels could be used as a scaffold for *in situ* generation of Ag NPs, which could subsequently be used as a colorimetric sensor for H₂O₂.²⁵

In this investigation, we show that pNIPAm-based microgels can be used as a scaffold for the generation and stabilization of CuSNPs; we hypothesize that the resultant microgels will be responsive to NIR exposure. Specifically, we propose an *in situ* synthetic route for the preparation of CuSNPs@pNIPAm-co-AAc hybrid microgels. Copper ions were enriched in the microgels through deprotonation of the pNIPAm-co-AAc microgels. CuSNPs were subsequently generated in the pNIPAm-co-AAc microgels utilizing a previously reported hydrothermal method.¹³ The hybrid materials were also shown to exhibit typical NIR absorption and photothermal properties. We go on to show that NIR excitation of the hybrid microgels could be used to kill HeLa cells. This concept can be further modified in the future to allow photothermal treatment of cancer cells and tumors.

Experimental section

Materials and methods

N-isopropylacrylamide (NIPAm) was purchased from TCI (Portland, OR) and puri-

fied through recrystallization from hexanes (ACS reagent grade, purchased from EMD, Gibbstown, OR). *N,N*-Methylenebisacrylamide (BIS), acrylic acid (AA), ammonium persulfate (APS), copper sulfate (CuSO_4), sodium hydroxide (NaOH), hydrochloric acid (HCl), sodium sulfide (Na_2S), 3-(4,5-dimethyl-2-thiazolyl)-2,5-diphenyl-2-H-tetrazolium bromide (MTT) and calcein-AM were supplied by Sigma-Aldrich (Oakville, ON). Microgel samples were lyophilized using a VirTis bench-top K-manifold Freeze Dryer (Stone Ridge, New York). Deionized (DI) water with a resistivity of 18.2 $\text{M}\Omega\cdot\text{cm}$ was obtained from a Milli-Q Plus system (Billerica, MA).

Characterization

UV-vis spectra of the as prepared CuSNPs@pNIPAm-co-AAc hybrid microgel solutions were collected using a 8452A diode array spectrophotometer (Hewlett Packard, USA). The size and morphology of CuSNPs@pNIPAm-co-AAc hybrid microgels was determined using a Hitachi H-7650 transmission electron microscope (TEM) at 200 kV accelerating voltage. X-ray photoelectron spectroscopy (XPS) was performed on a Kratos AXIS Ultra spectrometer equipped with a monochromated Al $\text{K}\alpha$ ($h\nu=1486.6$ eV) X-ray source (Kratos Analytical, Manchester, UK). Fourier transform infrared (FT-IR) spectra ($400\text{-}4000\text{ cm}^{-1}$) were recorded on a Nicolet Magna 750 FTIR Spectrometer and Nic-Plan FTIR Microscope (Nicolet, USA) with pure KBr as the background.

Synthesis of pNIPAm-co-AAc microgels

pNIPAm-co-AAc microgels were synthesized via surfactant-free, free radical precipitation polymerization, according to an established protocol.²⁵ The monomer, NIPAm (10.54 mmol), and the crosslinker, BIS (0.703 mmol), were fully dissolved in water (99 mL) with stirring in a beaker for 1 h. The mixture was then filtered through a 0.2 μm filter affixed to a 20 mL syringe into a 250 mL, 3-necked round bottom flask. The flask was then equipped with a thermometer, a condenser/ N_2 inlet/outlet, and a stir bar. The monomer solution was purged with N_2 gas for ~ 1 h while stirring and heating to 70 $^\circ\text{C}$. AAc (2.812 mmol) and APS (0.046 g in 1.0 mL water) was then added to the pre-heated solution, respectively. The reaction continued for 4 h. After cooling down,

the turbid solution was filtered through glass wool to remove any large aggregates. The coagulum was rinsed and the collected liquid was diluted to 100 mL. Aliquots of the microgel solution (33 mL) were centrifuged at a speed of 10 000 relative centrifugal force (rcf) at 20 °C for 45 min. The microgels were isolated and redispersed to their original volume (~33 mL) with DI water. This centrifugation/resuspension procedure was repeated 6 times. Finally, all of the centrifuged particles were combined into one tube and diluted to 30 mL with DI water for storage. We also calculated the percent yield by removing a 1 mL aliquot of solution from the final, purified 30 mL microgel solution. This aliquot was lyophilized and the resulting dried microgels weighed. The mass was subsequently multiplied by 30 (to get the mass of microgels in the 30 mL solution), which was compared to the mass of all the components (NIPAm, BIS, AAc) used to synthesize the microgels, and a percent yield determined. Using this approach, 80% yield was determined.

Synthesis of CuSNPs@pNIPAm-co-AAc hybrid microgels

Hybrid microgels were prepared using the hydrothermal reaction between Cu^{2+} and S^{2-} in the pNIPAm-co-AAc microgel networks.¹³ Briefly, the pH of 10 mL of the microgel solution from the above purification process was adjusted accordingly with addition of HCl and NaOH followed by equilibration for 1 h. The microgel solution was then washed by centrifugation and resuspension in DI water 6 times. Following the final centrifugation, the isolated microgels were resuspended in 10 mL CuSO_4 solution (500 mM in DI water) and incubated with gentle shaking overnight. This process of washing the microgels with DI water after exposure to the desired pH solutions was used because Cu^{2+} precipitates at high pH, which would make loading the microgels at high pH impossible. Therefore, by rinsing all the microgels with DI water, the pH of the Cu^{2+} loading step was constant for all experiments. The Cu^{2+} loaded microgels were then washed another 6 times by centrifugation and resuspension with DI water to remove any free Cu^{2+} . The purified Cu^{2+} loaded microgels (10 mL) and 75 mL of DI water were combined into a three-necked round bottom flask (250 mL) equipped with a thermometer, N_2 inlet and condenser. The solution was bubbled with N_2 for 1 h and heated to 90 °C, followed by the drop-wise addition of 175 μL Na_2S

solution (500 mM) within 2 min. After adding Na₂S, the reaction was allowed to proceed for 2 h and the color of mixture immediately changed from bluish to brick red, and gradually turned to dark green. Finally, the cooled solution was washed by centrifugation and resuspension in DI water 6 times to yield the purified CuSNPs@pNIPAm-co-AAc hybrid microgels. The concentrated, centrifuged microgels were diluted to a final volume of 85 mL in DI water.

Measurement of the photothermal performance

Solutions of CuSNPs@pNIPAm-co-AAc hybrid microgels of various concentrations (400, 800, and 1600 mg/L) were added to test tubes. A laser probe (808 nm, 2.0 W/cm⁻²) was fixed 5 cm away from the center of the test tube and the solution exposed to the laser for 10 min to evaluate the photothermal performance. The temperature change of the solution was recorded using a thermocouple probe.

Cytotoxicity of CuSNPs@pNIPAm-co-AAc hybrid microgels

Cytotoxicity was evaluated utilizing the MTT assay and human cervical carcinoma (HeLa) cells. HeLa cells were cultured in Dulbecco's Modified Eagle Medium (DMEM, Gibco) supplemented with 10% fetal bovine serum and 1% penicillin-streptomycin at 37 °C under 5% CO₂. The cells were then seeded into a 96-well plate (1×10⁴ cells/well) and incubated for 24 h. Afterwards, HeLa cells were incubated with different concentrations of CuSNPs@pNIPAm-co-AAc hybrid microgels for 24 h. After washing with PBS, cells were supplemented with 100 μL of DMEM and exposed to MTT (20 μL in PBS, 5 mg/mL) for 4 h. Subsequently, after removal of supernatant solution from each well, 150 μL of DMSO was added and the absorbance of the solution in each well was recorded by using a multi-mode microplate reader. Eight replicates were prepared for each treatment group.

Photothermal killing of HeLa cells with CuSNPs@pNIPAm-co-AAc hybrid microgels

The potential use of CuSNPs@pNIPAm-co-AAc hybrid microgels for photothermal therapy was assessed using HeLa cells and the MTT assay and calcein-AM (calcein acetoxymethyl ester) staining. For the MTT assay, HeLa cells were incubated in a 96-well culture plate (5×10⁵ cells/well) for 24 h at 37 °C under 5% CO₂ and washed

with PBS. Similarly, CuSNPs@pNIPAm-co-AAc hybrid microgels were added to the culture medium and incubated for 4 h at 37 °C, followed by exposure to the 808 nm laser with power density of 2 W/cm⁻² for 10 min at a fixed distance of 5 cm from the plate. A control experiment was performed on cells exposed to the laser but in the absence of the hybrid microgels. The cells continued to be cultured for other 20 h. Cell viability was then evaluated using the MTT assay and confocal microscopy. Calcein-AM was used to stain live cells, and then the confocal images were obtained.

Results and discussion

The synthetic route for generating CuSNPs@pNIPAm-co-AAc hybrid microgels is shown schematically in Figure 1. As we expected the protonation state of the pNIPAm-co-AAc microgels to change their ability to absorb Cu²⁺,²⁶ we evaluated how solution pH impacted the generation of CuSNPs in the microgels. To accomplish this, we adjusted the pH of the microgel solutions to above and below the pK_a for AAc (4.25) followed by exposure to Cu²⁺ solution.²⁷ We want to point out that at Cu²⁺ precipitates at high pH. Therefore microgels at all the investigated pH were washed with DI water via centrifugation/resuspension (see Experimental Section) prior to Cu²⁺ exposure to ensure that all the Cu²⁺ exposures were done at the same conditions without precipitation. The isolated microgels were then exposed to S²⁻ to form CuSNPs (as described in the Experimental Section) and the NIR absorption efficiency and water solubility was determined.

First, we evaluated how the solution pH impacted the Cu²⁺ absorption step by visually noting the microgel solubility. As can be seen in Figure S1, the microgels that were at pH 3.0 and 4.3 then washed with DI water (as detailed in the Experimental Section) and finally exposed to Cu²⁺ were found to agglomerate and attach to the wall of centrifuge tubes. Although, when the pH of the solution the microgels were exposed to before Cu²⁺ exposure increased, the microgels could be homogeneously dispersed in the aqueous solution. Figure S1 also showed that the color of the pNIPAm-co-AAc-Cu²⁺ microgel solution changed from white to cyan as the solution pH increased. We hypothesize that since the pK_a of AAc was ~4.25, when the solu-

tion pH was greater than 4.25, the deprotonated acids can absorb more Cu^{2+} . This is supported by previously reported results that demonstrated that protonated carboxylic acid groups are much less capable of forming complexes with Cu^{2+} than the salt form, resulting in the progressive decrease in the retention of Cu^{2+} at low pH.²⁸ Moreover, as the solution pH increased, the presence of free lone pair of electrons on nitrogen and deprotonated oxygen atoms, further facilitated the coordination of microgels with Cu^{2+} by the microgels.²⁹ Finally, the absorbance spectra for the CuSNPs@pNIPAm-co-AAc hybrid microgels that were loaded with Cu^{2+} at the various pHs were collected and used as a final determinant of the quality of the hybrid microgels; high absorbance in the NIR wavelength range is desirable. As can be seen in Figure 2a, the absorbance reaches a maximum when the microgels were loaded with Cu^{2+} at pH 8.5, with no further improvement as the solution pH was further increased. This result can be understood by considering that the microgels are nearly 100% deprotonated at pH 8.5, so a further increase in pH yields virtually no change in the charge density of the microgels, and hence should have minimal impact on the extent of Cu^{2+} uptake. We also investigated how the order of adding S^{2-} affected the resultant NIR absorption of the hybrid microgels. Conventionally, to synthesize CuSNPs with Cu^{2+} and S^{2-} , the ion mixing step is followed by solution heating.³⁰ However, in this investigation, we observed that heating the microgel solution first followed by addition of S^{2-} resulted in higher quality hybrid microgels, as can be seen from the stronger NIR absorbance in the UV-vis spectra in Figure 2b. Finally, we investigated how the concentration of S^{2-} impacted the optical properties of the CuSNPs@pNIPAm-co-AAc hybrid microgels, which revealed that 87.5 μmol was ideal, producing hybrid microgels with the highest NIR absorbance (Figure 2c and 2d). The hybrid microgels synthesized with an amount of S^{2-} higher than 87.5 μmol tended to aggregate and settle out of solution, resulting in a decrease in of NIR absorbance of the hybrid microgels.

The CuSNPs@pNIPAm-co-AAc hybrid microgels were well dispersed in water and can be stored in 4 °C for more than one month without precipitation. We also note that the solution of CuSNPs@pNIPAm-co-AAc hybrid microgels was dark green, while

solutions of pNIPAm-co-AAc microgels are typically clear, colorless, and slightly turbid. It is also worth noting that the CuSNPs prepared in the presence of the microgels were extremely stable, when compared to those prepared without the microgels (Figure S2). Specifically, CuSNPs prepared in the absence of microgels aggregated very quickly and precipitated, further showing the benefits of using the microgel structure to stabilize the CuSNPs. Therefore, for the rest of experiments in the manuscript, the CuSNPs@pNIPAm-co-AAc hybrid microgels were prepared by exposing the microgels to pH 8.5, followed by washing with DI water and exposure to Cu^{2+} , followed by washing with DI water, heating the solution, followed by adding 87.5 μmol of S^{2-} and a final washing with DI water.

The morphology of the CuSNPs@pNIPAm-co-AAc hybrid microgels was determined using the TEM imaging, as shown in Figure S3. The TEM images (Figure 3a and 3b, respectively) showed that the microgel scaffold exhibited a spherical shape with relatively low contrast and a diameter of ~ 700 nm, microgels. Within the microgel network, a total of ~ 40 - 50 CuSNPs with diameters of ~ 10 nm could be observed. The formation of crystalline CuSNPs inside the pNIPAm-co-AAc microgels was subsequently investigated by XRD. As can be seen in Figure 3c, the XRD pattern obtained from lyophilized microgels displayed a series of sharp peaks at 29.3° , 31.9° and 48.0° , which were in agreement with the lattice planes of CuSNPs (102), (103) and (110), respectively. These crystal characteristics of CuSNPs evidenced the formation of covellite CuS (hexagonal phase, JCPDS no. 06-0464).³¹ Figure 3d shows the XPS spectrum of CuSNPs incorporated in pNIPAm-co-AAc microgels, exhibiting two peaks at 931.6 eV and 951.7 eV, which were attributed to Cu 2p_{3/2} and Cu 2p_{1/2} respectively, while no such peaks were found in the XPS spectrum of the native microgels (Figure S4). The gap between the two peaks was 20.1 eV, confirming that the oxidation state of elementary copper in CuSNPs was +2.³¹ These characterizations demonstrated that the microgels could adequately serve as microreactors for the nucleation and growth of CuSNPs.

As mentioned above, pNIPAm microgels have generated significant interest due to their thermoresponsivity, which can be exploited for triggered drug delivery. Here, we

investigated the thermoresponsivity of the CuSNPs@pNIPAm-co-AAc hybrid microgels. As illustrated in Figure 4a, the pure copolymer microgels exhibited the expected thermoresponsivity. That is, as the solution temperature was increased above the microgel LCST (around 32 °C), the microgels scatter more light due to their collapse, as evidenced as an increased in absorbance measured from UV-vis spectroscopy. However, in the case of the hybrid microgels, there was no such behavior observed up to a solution temperature of 50 °C. While copolymerization of AAc with pNIPAm is well known to increase its LCST,³² thermoresponsivity is observed as the solution temperature approaches 40 °C. In the case of the hybrid microgels synthesized here, no significant thermoresponsivity was observed even up to 50 °C. Furthermore, the lack of thermoresponsivity from similar hybrid polymers has also reported in previous studies.^{18, 25, 33} Therefore, we hypothesize that the presence of CuSNPs in the microgels is stabilizing the polymers against temperature-induced collapse, although this has not been studied in detail here.

FT-IR analysis was also employed to investigate the interaction between the pNIPAm-co-AAc microgels and CuSNPs, and to shed some light on the loss of thermoresponsivity for the hybrid microgels. As shown in Figure 4c, the pure pNIPAm-co-AAc microgels, exhibited a peak at 1714 cm⁻¹, which was attributed to free carboxyl group (-COOH), according to previous reports.³⁴ Whereas, for the CuSNPs@pNIPAm-co-AAc hybrid microgels, this characteristic peak was absent, indicating that all of carboxyl groups were occupied and/or deprotonated. We also observed that the characteristic peak from the deprotonated carboxyl group -COO⁻ at 1569 cm⁻¹ in the hybrid microgels was also absent.³⁵ Taken together, we concluded that the carboxyl groups were interacting with the CuSNPs, allowing them to be immobilized in the microgel network. However, as can be seen in the TEM images, there's significant space between CuSNPs in the microgel network, revealing that the microgels were not fully loaded with CuSNPs. Therefore, the carboxyl groups are also likely to have unreacted Cu²⁺ coordinated. While more S²⁻ could be added to react with this extra Cu²⁺, this would lead to the aggregation of the hybrid microgels, as shown in Figure 3d. Additionally, the peaks around 1534 cm⁻¹ were ascribed to the

amide II (-NH) of NIPAm moieties due to the bending of N-H bonds,³⁶ and the 1648 cm^{-1} band represents the stretching vibration band of amide I (-C=O).³⁷ The ratio of peak intensity at 1534 and 1648 cm^{-1} to other peaks, significantly increased after generating the CuSNPs, suggesting the interaction between amide and Cu^{2+} /CuSNPs. The shift of the broad band from 3310 to 3295 cm^{-1} , which was assigned to the hydrogen-bonded N-H stretching,³⁸ further indicated this underlying interaction. Together, the FT-IR results revealed that the loss of thermoresponsivity of pNIPAm in this system was likely a result of the disruption of hydrogen bonds by Cu^{2+} /CuSNPs. Therefore, it was concluded that the *in situ* CuSNPs synthesis presented here was not suitable to generate hybrid microgels that were thermoresponsive. While this is the case, the use of microgels to stabilize the CuSNPs is important, and the hybrid microgels could still be very useful for photothermal therapy. If thermoresponsive hybrid microgels are desired, there is the possibility of simply mixing the CuSNPs with the already synthesized microgels,^{18, 23} although there are other challenges associated with this approach.

The NIR photothermal performance of the CuSNPs@pNIPAm-co-AAc hybrid microgels was investigated using laser irradiation (808 nm) with a power density of 2 W/cm^2 for 10 min. As shown in Figure 5a, the microgels without CuSNPs were not capable of converting NIR light energy to heat and only a 3 °C increase in solution temperature was observed after 10 min irradiation. As for the hybrid microgels, the incorporated CuSNPs were capable of absorbing NIR irradiation and generating heat. Specifically, solutions of 400 to 1600 $\mu\text{g}/\text{mL}$ CuSNPs@pNIPAm-co-AAc hybrid microgels, were shown to increase the solution temperature from 9 to 18 °C after 10 min NIR irradiation.

Next, the cytotoxicity of CuSNPs@pNIPAm-co-AAc hybrid microgels was investigated. HeLa cells were incubated with different concentrations of hybrid microgels for 24 h, and were subsequently characterized using a standard MTT assay to assess their viability. As shown in Figure 5b, relatively high cell viability (> 80%) could be achieved even after exposure to microgels solutions with concentrations as high as 400 $\mu\text{g}/\text{mL}$, showing low cytotoxicity of the prepared photothermal materials. Previ-

ous studies have confirmed that pNIPAm microgels and their derivatives,³⁹⁻⁴⁰ including pNIPAm-co-AAc microgels,³⁹ possessed relatively low cytotoxicity. Also, CuSNPs are known for their excellent biocompatibility.⁵ Thus, the lack of cytotoxicity of the combined materials was not a surprising result.

Finally, the ability of the CuSNPs@pNIPAm-co-AAc hybrid microgels to photothermally trigger cell death was evaluated. HeLa cells were treated with different concentrations of CuSNPs@pNIPAm-co-AAc hybrid microgels for 4 h at 37 °C and were subsequently exposed to a 808 nm laser with a power density of 2 W/cm² for 10 min. As shown in Figure 5c and 5d, the *in vitro* cytotoxicity assay using the MTT method and calcein staining showed that there were no obvious changes in viability of HeLa cells when exposed to CuSNPs@pNIPAm-co-AAc hybrid microgels. The viability was similar to what we observed for HeLa cells exposed to pNIPAm-co-AAc microgels without CuSNPs. Furthermore, exposure of the HeLa cells to laser irradiation in the absence of CuSNPs@pNIPAm-co-AAc hybrid microgels also retained approximately 90% viability of cells. However, when the HeLa cells were incubated with the CuSNPs@pNIPAm-co-AAc hybrid microgels and exposed to laser irradiation, significant loss in viability was observed. Cell death was also increased when the concentration of the CuSNPs@pNIPAm-co-AAc hybrid microgels was increased. Specifically, less than 10% cells survived when the cells were irradiated by a 2 W/cm² NIR laser for 10 min, when the dosage of the CuSNPs@pNIPAm-co-AAc hybrid microgels increased to 400 µg/mL.

Conclusions

An *in situ* approach for generating CuSNPs@pNIPAm-co-AAc hybrid microgels was presented and optimized. The NIR absorbance of the resultant materials, and their photothermal capacity was investigated. Using the optimum synthetic conditions discovered as part of this work, we found that solutions containing 1600 µg/mL CuSNPs@pNIPAm-co-AAc hybrid microgels could yield a temperature increase of 18 °C after 10 min NIR irradiation. We also conducted FT-IR analysis to elucidate the interactions that are resulting in Cu²⁺/CuSNPs incorporation into the microgels; these

experiments also shed light on the loss of thermoresponsivity of the CuSNPs@pNIPAm-co-AAc hybrid microgels. Finally, we went on to show that the cytotoxicity of the CuSNPs@pNIPAm-co-AAc hybrid microgels was low, although they could be made to kill cells upon exposure to NIR laser light, which is presumably a result of the photothermal effect. Hence, the microgels themselves are simply serving as a stabilization matrix, which is necessary, as CuS nanoparticles that are not stabilized tend to aggregate and become useless. While this work can serve as the basis for the *in situ* generation of other nanoparticles in microgels for various applications, there are also other potential uses of these materials. Specifically, this work can be extended to incorporate the CuSNPs@pNIPAm-co-AAc hybrid microgels into a thermoresponsive hydrogel matrix and can serve as the photothermal moiety to trigger hydrogel collapse and small molecule release.

Acknowledgements

MJS acknowledges funding from the University of Alberta (the Department of Chemistry and the Faculty of Science), the Natural Sciences and Engineering Research Council of Canada (NSERC), the Canada Foundation for Innovation (CFI), the Alberta Advanced Education & Technology Small Equipment Grants Program (AET/SEGP), Grand Challenges Canada and IC-IMPACTS. XZ and TS acknowledge support from the National Natural Science Foundation of China (Grant No. 21727815), the Beijing Municipal Science and Technology Commission (z131102002813058), the Natural Science Foundation of Beijing (2184107), Beijing Natural Science Foundation (2184107) and the Fundamental Research Funds for the Central Universities (FRF-TP-15-096A1).

Supporting Information Available: [Photographs of the hybrid microgel preparation; TEM image for the hybrid microgels; XRD spectrum for the native microgels without CuSNPs]

References

- (1) Nioka, S.; Chance, B. NIR Spectroscopic Detection of Breast Cancer. *Technol. Cancer Res. T.* **2005**, *4*, 497-512.
- (2) Cheng, L.; Wang, C.; Feng, L. Z.; Yang, K.; Liu, Z. Functional Nanomaterials for Phototherapies of Cancer. *Chem. Rev.* **2014**, *114*, 10869-10939.
- (3) Lim, E. K.; Kim, T.; Paik, S.; Haam, S.; Huh, Y. M.; Lee, K. Nanomaterials for Theranostics: Recent Advances and Future Challenges. *Chem. Rev.* **2015**, *115*, 327-394.
- (4) Zhang, L.; Li, Y. C.; Jin, Z. X.; Yu, J. C.; Chan, K. M. An NIR-Triggered and Thermally Responsive Drug Delivery Platform through DNA/Copper Sulfide Gates. *Nanoscale* **2015**, *7*, 12614-12624.
- (5) Meng, X. D.; Liu, Z. Q.; Cao, Y.; Dai, W. H.; Zhang, K.; Dong, H. F.; Feng, X. Y.; Zhang, X. J. Fabricating Aptamer-Conjugated Pegylated-MoS₂/Cu_{1.8}S Theranostic Nanoplatfrom for Multiplexed Imaging Diagnosis and Chemo-Photothermal Therapy of Cancer. *Adv. Funct. Mater.* **2017**, *27*.
- (6) Cao, Y.; Dong, H. F.; Yang, Z.; Zhong, X. M.; Chen, Y.; Dai, W. H.; Zhang, X. J. Aptamer-Conjugated Graphene Quantum Dots/Porphyrin Derivative Theranostic Agent for Intracellular Cancer-Related Microrna Detection and Fluorescence-Guided Photothermal/Photodynamic Synergetic Therapy. *ACS Appl. Mater. Inter.* **2017**, *9*, 159-166.
- (7) Yue, C.; Liu, P.; Zheng, M.; Zhao, P.; Wang, Y.; Ma, Y.; Cai, L. IR-780 Dye Loaded Tumor Targeting Theranostic Nanoparticles for NIR Imaging and Photothermal Therapy. *Biomaterials.* **2013**, *34*, 6853-6861.
- (8) Huschka, R.; Zuloaga, J.; Knight, M. W.; Brown, L. V.; Nordlander, P.; Halas, N. J. Light-Induced Release of DNA from Gold Nanoparticles: Nanoshells and Nanorods. *J. Am. Chem. Soc.* **2011**, *133*, 12247-12255.
- (9) Wang, Y.; Wang, K.; Zhang, R.; Liu, X.; Yan, X.; Wang, J.; Wagner, E.; Huang, R. Synthesis of Core-Shell Graphitic Carbon@Silica Nanospheres with Dual-Ordered Mesopores for Cancer-Targeted Photothermochemotherapy. *ACS Nano* **2014**, *8*, 7870-7879.
- (10) Huang, X. Q.; Tang, S. H.; Mu, X. L.; Dai, Y.; Chen, G. X.; Zhou, Z. Y.; Ruan, F. X.; Yang, Z. L.; Zheng, N. F. Freestanding Palladium Nanosheets with Plasmonic and Catalytic Properties. *Nat. Nanotechnol.* **2011**, *6*, 28-32.
- (11) Luther, J. M.; Jain, P. K.; Ewers, T.; Alivisatos, A. P. Localized Surface Plasmon Resonances Arising from Free Carriers in Doped Quantum Dots. *Nat. Mater.* **2011**, *10*, 361-366.
- (12) Han, L.; Zhang, Y.; Chen, X. W.; Shu, Y.; Wang, J. H. Protein-Modified Hollow Copper Sulfide Nanoparticles Carrying Indocyanine Green for Photothermal and Photodynamic Therapy. *J. Mater. Chem. B* **2016**, *4*, 105-112.
- (13) Zhang, C.; Fu, Y.Y.; Zhang, X.; Yu, C.; Zhao, Y.; Sun, S.K. BSA-Directed Synthesis of CuS Nanoparticles as a Biocompatible Photothermal Agent for Tumor Ablation *in vivo*. *Dalton T.* **2015**, *44*, 13112-13118.
- (14) Zhou, M.; Song, S.; Zhao, J.; Tian, M.; Li, C. Theranostic CuS Nanoparticles Targeting Folate Receptors for PET Image-Guided Photothermal Therapy. *J. Mater. Chem. B* **2015**, *3*, 8939-8948.
- (15) Stuart, M. A. C.; Huck, W. T. S.; Genzer, J.; Muller, M.; Ober, C.; Stamm, M.; Sukhorukov, G. B.; Szleifer, I.; Tsukruk, V. V.; Urban, M.; Winnik, F.; Zauscher, S.; Luzinov, I.; Minko, S. Emerging Applications of Stimuli-Responsive Polymer Materials. *Nat. Mater.* **2010**, *9*, 101-113.
- (16) Mendes, P. M. Stimuli-Responsive Surfaces for Bio-Applications. *Chem. Soc. Rev.* **2008**, *37*,

2512-2529.

(17) Jia, H.; Roa, R.; Angioletti-Uberti, S.; Henzler, K.; Ott, A.; Lin, X.; Möser, J.; Kochovski, Z.; Schnegg, A.; Dzubiella, J.; Ballauff, M.; Lu, Y. Thermosensitive Cu₂O-pNIPAM Core-Shell Nanoreactors with Tunable Photocatalytic Activity. *J. Mater. Chem. A* **2016**, *4*, 9677-9684.

(18) Lu, N.; Liu, J.; Li, J.; Zhang, Z.; Weng, Y.; Yuan, B.; Yang, K.; Ma, Y. Tunable Dual-Stimuli Response of a Microgel Composite Consisting of Reduced Graphene Oxide Nanoparticles and Poly(N-Isopropylacrylamide) Hydrogel Microspheres. *J. Mater. Chem. B* **2014**, *2*, 3791-3798.

(19) Li, X.; Serpe, M. J. Understanding the Shape Memory Behavior of Self-Bending Materials and Their Use as Sensors. *Adv. Funct. Mater.* **2016**, *26*, 3282-3290.

(20) Wu, X.; Pelton, R. H.; Hamielec, A. E.; Woods, D. R.; McPhee, W. The Kinetics of Poly(N-Isopropylacrylamide) Microgel Latex Formation. *Colloid Polym. Sci.* **1994**, *272*, 467-477.

(21) Hoare, T.; Pelton, R. Highly pH and Temperature Responsive Microgels Functionalized with Vinylacetic Acid. *Macromolecules* **2004**, *37*, 2544-2550.

(22) Zhang, J.; Xu, S.; Kumacheva, E. Polymer Microgels: Reactors for Semiconductor, Metal, and Magnetic Nanoparticles. *J. Am. Chem. Soc.* **2004**, *126*, 7908-7914.

(23) Das, M.; Sanson, N.; Fava, D.; Kumacheva, E. Microgels Loaded with Gold Nanorods: Photothermally Triggered Volume Transitions under Physiological Conditions. *Langmuir* **2007**, *23*, 196-201.

(24) Gao, Y. F.; Wong, K. Y.; Ahiabu, A.; Serpe, M. J. Sequential and Controlled Release of Small Molecules from Poly(N-Isopropylacrylamide) Microgel-Based Reservoir Devices. *J. Mater. Chem. B* **2016**, *4*, 5144-5150.

(25) Han, D.; Zhang, Q. M.; Serpe, M. J. Poly (N-Isopropylacrylamide)-co-(Acrylic Acid) Microgel/Ag Nanoparticle Hybrids for the Colorimetric Sensing of H₂O₂. *Nanoscale* **2015**, *7*, 2784-2789.

(26) Cheng, J. J.; Shan, G. R.; Pan, P. J. Temperature and pH-Dependent Swelling and Copper(II) Adsorption of Poly(N-Isopropylacrylamide) Copolymer Hydrogel. *RSC Adv.* **2015**, *5*, 62091-62100.

(27) Yan, H.; Dai, J.; Yang, Z.; Yang, H.; Cheng, R. S. Enhanced and Selective Adsorption of Copper(II) Ions on Surface Carboxymethylated Chitosan Hydrogel Beads. *Chem. Eng. J.* **2011**, *174*, 586-594.

(28) Marinsky, J. A.; Anspach, W. M. Complexation of Copper(II) by a Polymethacrylic Acid Gel. *J. Phys. Chem.* **1975**, *79*, 439-444.

(29) Akl, M. A.; Sarhan, A. A.; Shoueir, K. R.; Atta, A. M. Application of Crosslinked Ionic Poly(Vinyl Alcohol) Nanogel as Adsorbents for Water Treatment. *J. Disper. Sci. Technol.* **2013**, *34*, 1399-1408.

(30) Zhou, M.; Zhang, R.; Huang, M. A.; Lu, W.; Song, S. L.; Melancon, M. P.; Tian, M.; Liang, D.; Li, C. A Chelator-Free Multifunctional [Cu-64]CuS Nanoparticle Platform for Simultaneous Micro-PET/CT Imaging and Photothermal Ablation Therapy. *J. Am. Chem. Soc.* **2010**, *132*, 15351-15358.

(31) Cho, K.; Han, S. H.; Suh, M. P. Copper-Organic Framework Fabricated with CuS Nanoparticles: Synthesis, Electrical Conductivity, and Electrocatalytic Activities for Oxygen Reduction Reaction. *Angew. Chem. Int. Edit.* **2016**, *55*, 15301-15305.

(32) Zhang J.; Chu L. Y.; Li Y. K.; Lee Y. M. Dual Thermo- and pH-Sensitive Poly(N-isopropylacrylamide-co-acrylic acid) Hydrogels with Rapid Response Behaviors. *Polymer* **2007**, *48*, 1718-1728.

- (33) Dong, Y.; Ma, Y.; Zhai, T. Y.; Shen, F. G.; Zeng, Y.; Fu, H. B.; Yao, J. N. Silver Nanoparticles Stabilized by Thermoresponsive Microgel Particles: Synthesis and Evidence of an Electron Donor-Acceptor Effect. *Macromol. Rapid. Comm.* **2007**, *28*, 2339-2345.
- (34) Yamashita, K.; Nishimura, T.; Nango, M. Preparation of IPN-Type Stimuli Responsive Heavy-Metal-Ion Adsorbent Gel. *Polym. Advan. Technol.* **2003**, *14*, 189-194.
- (35) Shukla, N. B.; Madras, G. Reversible Swelling/Deswelling Characteristics of Ethylene Glycol Dimethacrylate Cross-Linked Poly(Acrylic Acid-co-Sodium Acrylate-Co-Acrylamide) Superabsorbents. *Ind. Eng. Chem. Res.* **2011**, *50*, 10918-10927.
- (36) Zhang, Y. Y.; Yarin, A. L. Stimuli-Responsive Copolymers of N-Isopropyl Acrylamide with Enhanced Longevity in Water for Micro- and Nanofluidics, Drug Delivery and Non-Woven Applications. *J. Mater. Chem.* **2009**, *19*, 4732-4739.
- (37) Depciuch, J.; Sowa-Kucma, M.; Nowak, G.; Dudek, D.; Siwek, M.; Styczen, K.; Parlinska-Wojtan, M. Phospholipid-Protein Balance in Affective Disorders: Analysis of Human Blood Serum Using Raman and FTIR Spectroscopy. A Pilot Study. *J. Pharmaceut. Biomed.* **2016**, *131*, 287-296.
- (38) Park, J.; Hochstrasser, R. M. Multidimensional Infrared Spectroscopy of a Peptide Intramolecular Hydrogen Bond. *Chem. Phys.* **2006**, *323*, 78-86.
- (39) Zhang, W. J.; Mao, Z. W.; Gao, C. Y. Preparation of TAT Peptide-Modified Poly(N-Isopropylacrylamide) Microgel Particles and Their Cellular Uptake, Intracellular Distribution, and Influence on Cytotoxicity in Response to Temperature Change. *J. Colloid Interf. Sci.* **2014**, *434*, 122-129.
- (40) Das, M.; Mardyani, S.; Chan, W. C. W.; Kumacheva, E. Biofunctionalized pH-Responsive Microgels for Cancer Cell Targeting: Rational Design. *Adv. Mater.* **2006**, *18*, 80-83.

Figure caption

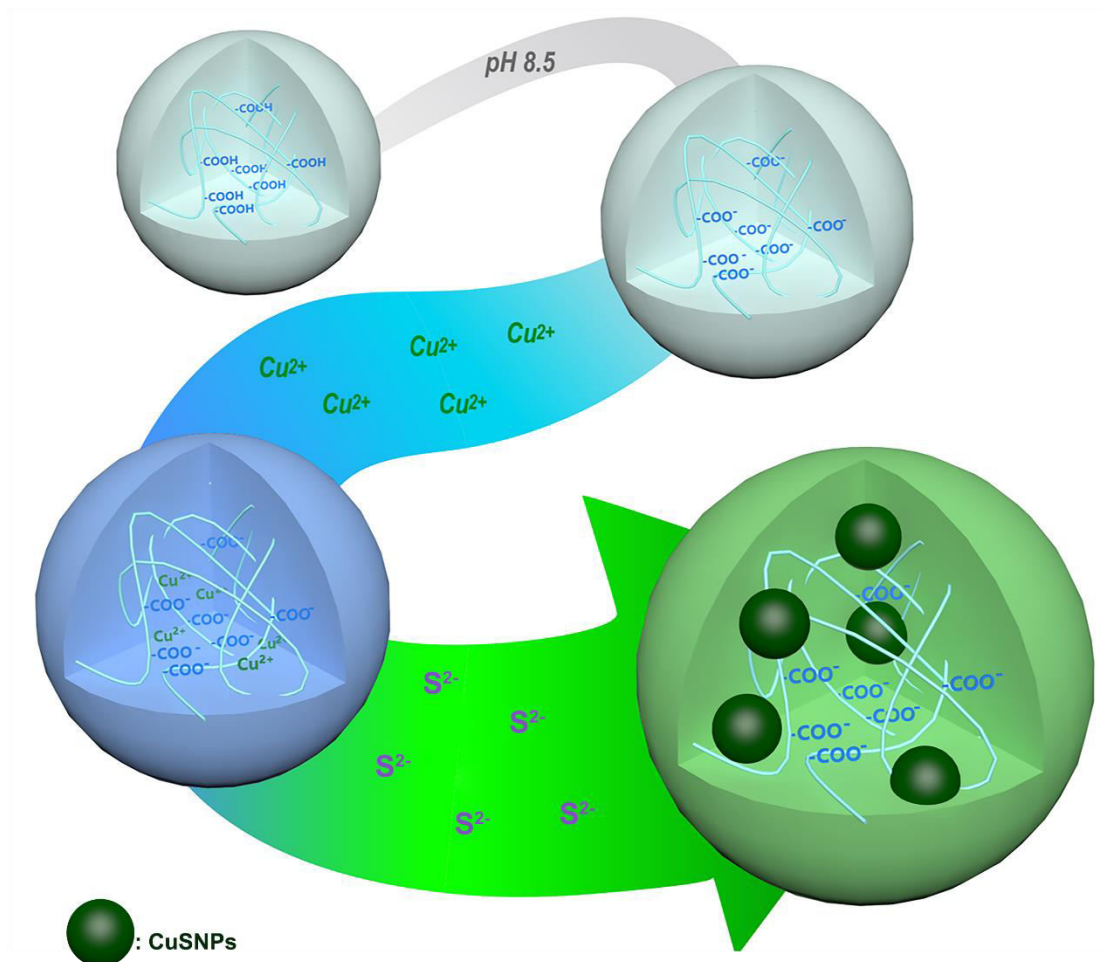


Figure 1. Schematic illustration of the generation of CuSNPs@pNIPAm-co-AAc hybrid microgels.

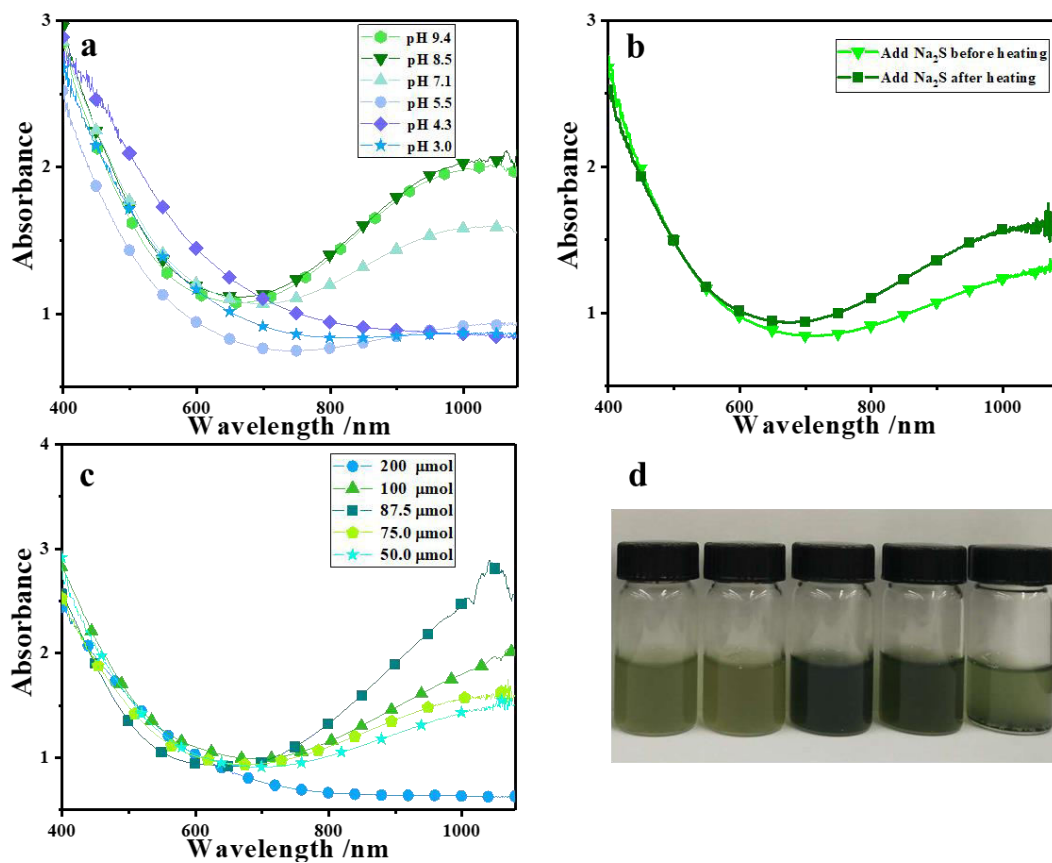


Figure 2. UV-vis spectra for CuSNPs@pNIPAm-co-AAc hybrid microgels synthesized: a) at different microgel solution pH before Cu^{2+} loading, b) using different order of S^{2-} addition, and c) using different amounts of added S^{2-} ; d) photograph of CuSNPs@pNIPAm-co-AAc hybrid microgels prepared using the various amounts of S^{2-} (from left to right: 50.0, 75.0, 87.5, 100, and 200 μmol).

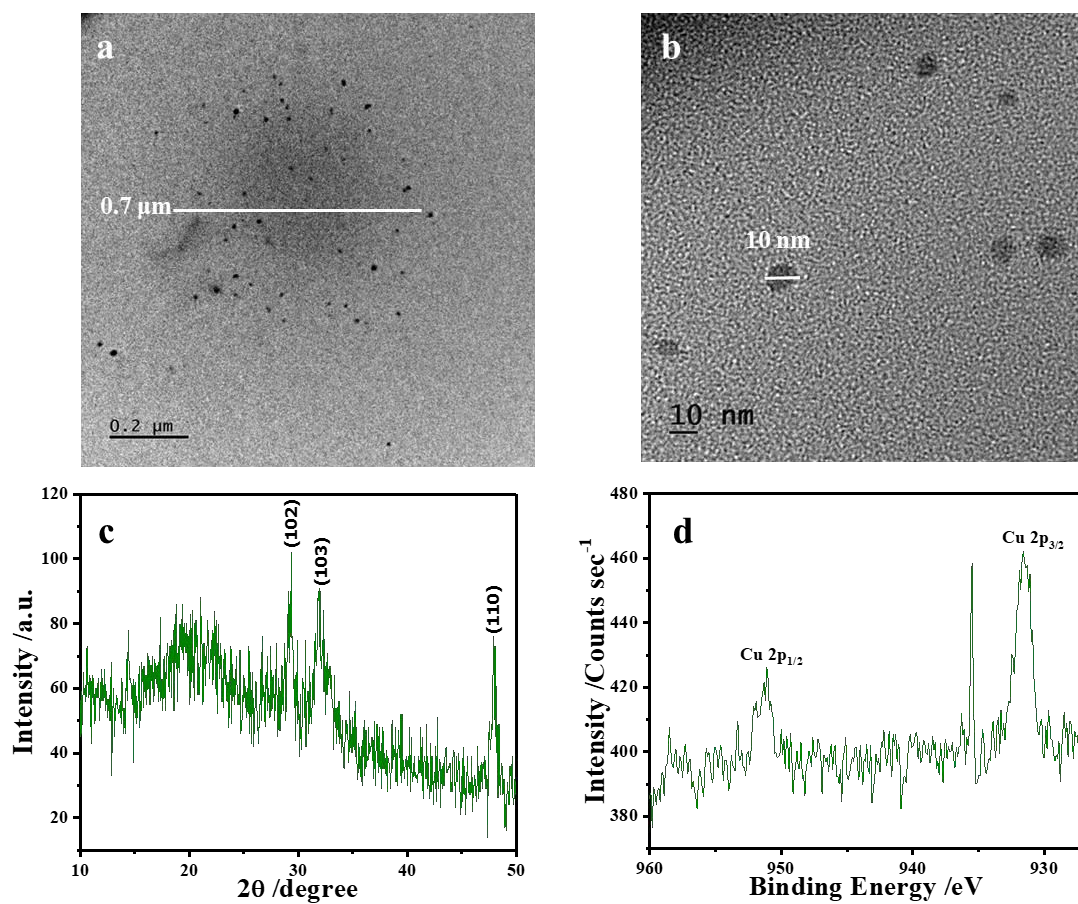


Figure 3. a) and b) TEM images of the CuSNPs@pNIPAm-co-AAc hybrid microgels and CuSNPs, respectively; c) X-ray diffraction pattern of CuSNPs@pNIPAm-co-AAc hybrid microgels; and d) X-ray photoelectron spectroscopy spectrum of CuSNPs@pNIPAm-co-AAc hybrid microgels.

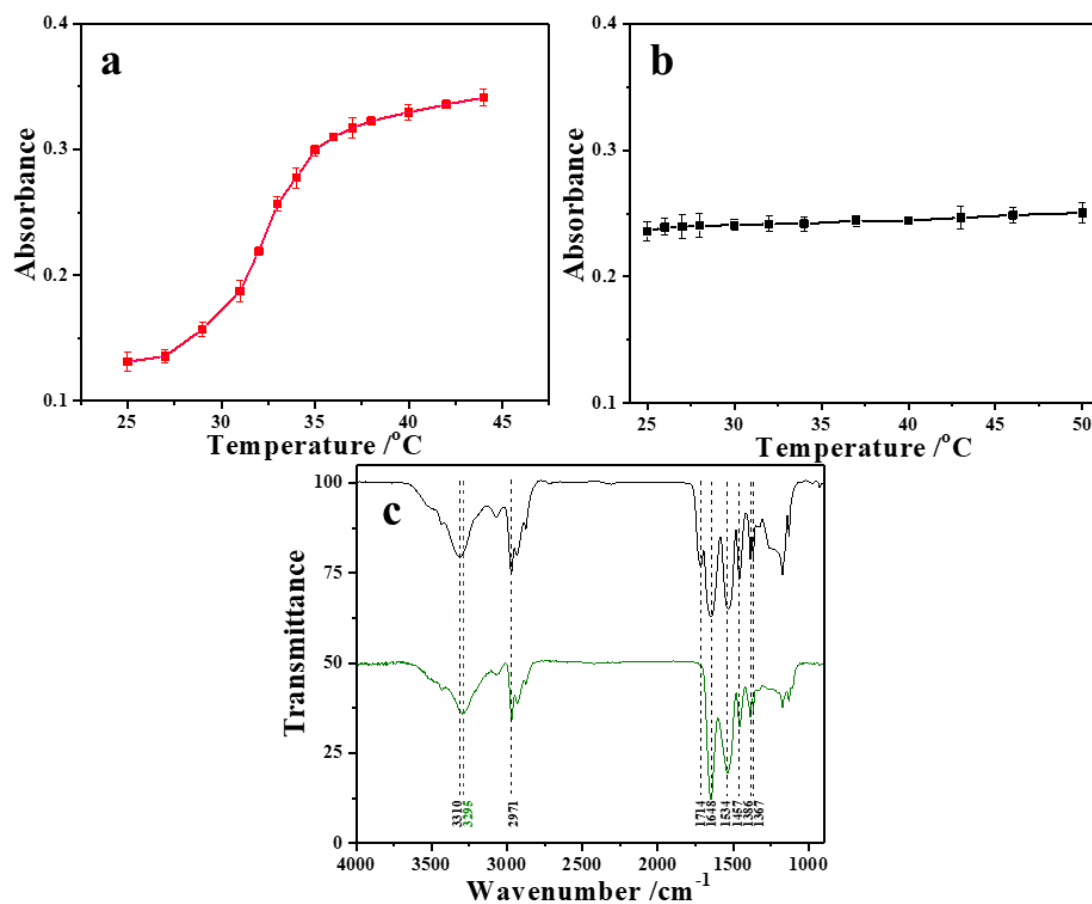


Figure 4. The maximum absorbance at 500 nm as a function of temperature for aqueous solutions of a) pNIPAm-co-AAc microgels, and b) CuSNPs@pNIPAm-co-AAc hybrid microgels. Data points are average values obtained from 3 independent measurements, while the error bars indicate the standard deviation of the mean. c) FT-IR spectra of the (black, top) pNIPAm-co-AAc microgels and the (green, bottom) CuSNPs@pNIPAm-co-AAc hybrid microgels.

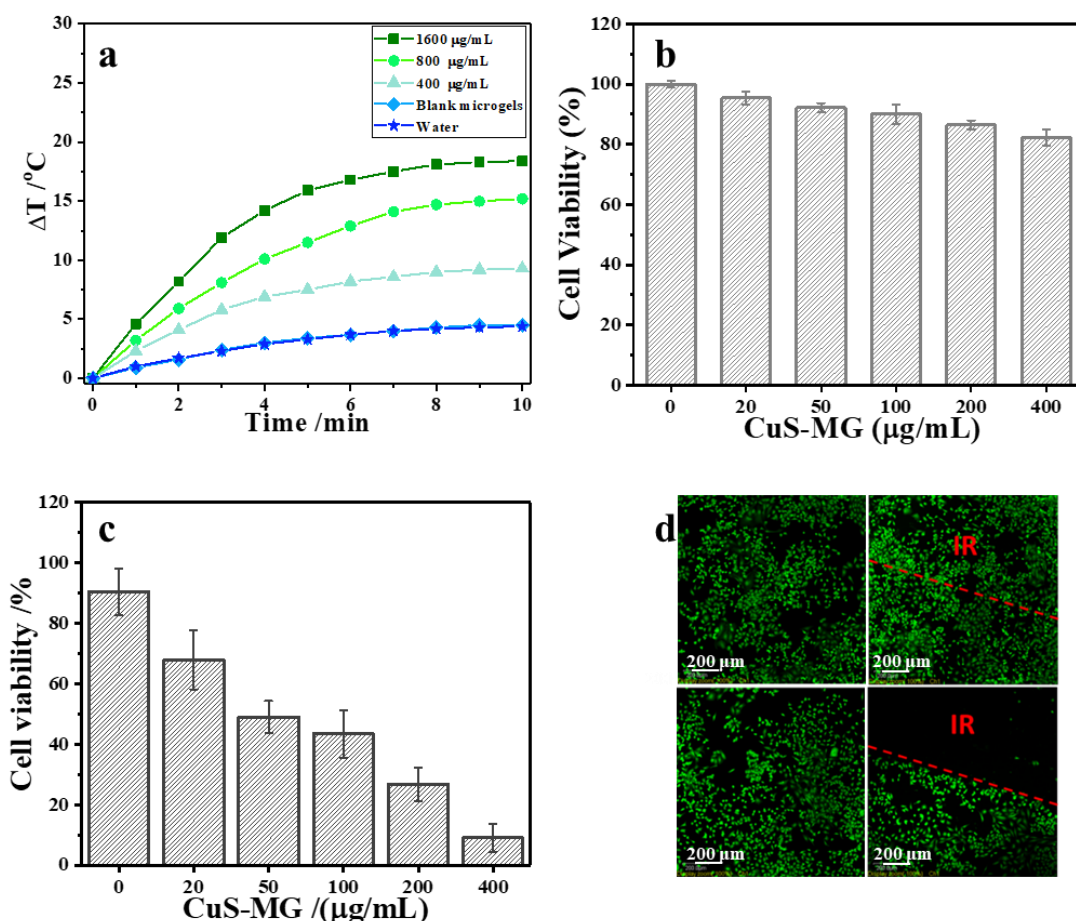


Figure 5. a) The photothermal heating curves of DI water, pNIPAm-co-AAc microgels and the CuSNPs@pNIPAm-co-AAc hybrid microgels at the indicated concentrations after exposure to a 808 nm laser with a power density of 2 W/cm² for the indicated times; b) the relative viability of HeLa cells before and after treatment with the indicated concentrations of CuSNPs@pNIPAm-co-AAc hybrid microgels; c) the relative viability of HeLa cells treated with the indicated concentrations of CuSNPs@pNIPAm-co-AAc hybrid microgels after exposure to a 808 nm laser for 10 min. Data in b) and c) are averages obtained from eight replicate experiments, while the error bars indicate the standard deviation of the mean. d) Fluorescence microscopy images of HeLa cells stained with calcein-AM (live cells were fluorescent). (Upper

row) HeLa cells not incubated with CuSNPs@pNIPAm-co-AAc hybrid microgels (left) before and (right) after exposure to the 808 nm laser; (bottom panel) HeLa cells incubated with CuSNPs@pNIPAm-co-AAc hybrid microgels (400 $\mu\text{g}/\text{mL}$) (left) before and (right) after exposure to the 808 nm laser.

TOC

